

Research Article

Synthesis of Titanium Oxide Nanoparticles Using Root Extract of *Kniphofia foliosa* as a Template, Characterization, and Its Application on Drug Resistance Bacteria

Eneyew Tilahun Bekele,¹ Bedasa Abdisa Gonfa^{ID},¹ Osman Ahmed Zelekew^{ID},² Hadgu Hailekiros Belay,¹ and Fedlu Kedir Sabir^{ID}¹

¹Department of Applied Chemistry, School of Applied Natural Science, Adama Science and Technology University, P.O. Box 1888, Adama, Ethiopia

²Department of Materials Science and Engineering, School of Chemical, Mechanicals and Materials Engineering, Adama Science and Technology University, P.O. Box 1888, Adama, Ethiopia

Correspondence should be addressed to Fedlu Kedir Sabir; fedluked130@gmail.com

Received 25 September 2019; Revised 26 February 2020; Accepted 3 April 2020; Published 5 May 2020

Academic Editor: David Cornu

Copyright © 2020 Eneyew Tilahun Bekele et al. This is an open access article distributed under the Creative Commons Attribution License, which permits unrestricted use, distribution, and reproduction in any medium, provided the original work is properly cited.

Biogenic methods of synthesis of nanoparticles (NPs) using plant extracts have been given a great attention due to its nontoxicity and environmental friendliness. In this study, TiO₂ NPs were synthesized from titanium tetrabutoxide and extract of root of *Kniphofia foliosa*. NPs of TiO₂ were biosynthesized at different volume compositions of titanium tetrabutoxide to the plant extract with a ratio of 1:2, 1:1, and 2:1, respectively. These green synthesized NPs of TiO₂ were characterized by thermogravimetric analysis (TGA/DTA), X-ray diffraction (XRD), scanning electron microscope-energy dispersive X-ray spectroscopy (SEM-EDS), transmission electron microscopy (TEM), ultraviolet-visible spectroscopy (UV-Vis), and Fourier transform infrared (FTIR) spectroscopy. TGA/DTA analysis has confirmed that the synthesized NPs of TiO₂ were stable above the temperature of 500°C. The sharp and intense peaks at 2θ values of 25.3, 38.0, 47.9, 53.2, 54.8862, 62.7, 70.2, and 75.0 have confirmed formation of crystalline NPs of TiO₂ in the sample of 1:1 and 2:1 ratios, and less crystalline samples for TiO₂ NPs prepared in a 1:2 ratio. Comparison between FT-IR absorption bands of the plant extract and that of calcined NPs of TiO₂ confirmed the purity of synthesized nanomaterials, except unavoidable adsorption of moisture on the surface of TiO₂ NPs in an open air. The antibacterial activity of biosynthesized TiO₂ NPs and that of ethanolic root extract of *Kniphofia foliosa* was investigated via the disc diffusion method against human pathogen bacteria strains of *Staphylococcus aureus*, *Escherichia coli*, *Klebsiella pneumonia*, and *Streptococcus pyogenes*. Among the different ratios, TiO₂ (1:1) NP shows better performance towards Gram-negative bacteria due to its smaller average crystalline size and uniform morphology observed in SEM image relative to the other two ratios of TiO₂ NPs. Antibacterial activity of the ethanolic root extract of *Kniphofia foliosa* itself showed better performance towards Gram-negative bacteria than NPs of TiO₂ that might be due to antibacterial activity of residue of ethanol left with the plant extract.

1. Introduction

The development of reliable experimental protocols for the synthesis of nanoparticles over a range of chemical compositions, sizes, and high monodispersity is one of the challenging issues in the current nanotechnology [1].

Synthesis of metal and metal oxide nanoparticles is a current field of material chemistry that has been attracted considerable interest due to the applications in vast fields such as in air and water purification, medicine, antimicrobial, information technology, photocatalytic, antimicrobial, energy reservoirs, and biosensors. Some metal nanoparticles owing

to unique properties such as gold and silver are getting synthesized through green method [2, 3] for antimicrobial activities. Leaf extracts of *Artemisia vulgaris* [4] and aerial parts of *Callistemon citrinus* plant extracts [5] were used in the synthesis of silver NPs for antibacterial and antimalarial applications, respectively. Towards this end, TiO_2 NPs also were more useful in the field of chemistry and nanomedicine as a result of their unique antibacterial and antimicrobial properties as well as their chemical stability. TiO_2 NPs are incorporated in cosmetics whereby creams and ointments are prepared having these nanoparticles to prevent skin aging and sunburns [6]. Successful applications of TiO_2 NPs are due to their increased surface area, which contributes to an increase in surface energy thereby enhancing their microbial and bacterial inhibition. TiO_2 NPs have been found to be useful in treating microbial and bacterial infection diseases; thus, biosynthesis of these nanoparticles could help in dealing with bacterial infections, which have become a menace due to their resistance to available medications [7–9]. Several methods have been employed in the synthesis of TiO_2 NPs and other metal and metal oxide NPs which include chemical and physical means with the former being the one mostly practiced industrially. These methods however have their own demerits as they require high temperatures, are potentially hazardous, are not safe to the natural environment, incorporate toxic chemicals as a reducing and capping agent during synthesis process, and at same time, are expensive [10, 11].

It has been reported that TiO_2 NPs were produced by the reaction between latex of *Jatropha curcas* leaves and $\text{TiO}(\text{OH})_2$. XRD and TEM revealed that the size of synthesized TiO_2 NPs was in the range of 100–200 nm. FTIR spectrum analysis of latex-capped TiO_2 NPs showed the presence of capping/stabilizing agents like protein/peptide material, which also prevents the nanoparticles from agglomeration [12]. It was also reported that TiO_2 NPs were synthesized using aqueous extracts of *Eclipta prostrata* leaves as a biotemplating agent. The obtained TiO_2 NPs were spherical in shape, their size ranged from 36 nm to 68 nm, and the calculated average crystalline size of biosynthesized TiO_2 NPs was estimated as 49.5 nm [13]. Previously TiO_2 NPs were biosynthesized using rice straw powder as biotemplate with titanium tetrakisopropoxide aqueous solution and acetic acid. The average crystalline size of the biosynthesized TiO_2 NPs was in the range of 10–20 nm [14]. Again, TiO_2 NPs were produced using an aqueous extract of *Psidium guajava* leaf and $\text{TiO}(\text{OH})_2$ precursor. The XRD pattern of the synthesized TiO_2 NPs showed the presence of both anatase (110) and rutile (111) crystallographic structures. The calculated average crystalline size of biosynthesized TiO_2 NPs was found to be 32.58 nm [15]. Plant extracts may act both as reducing and stabilizing agents in the synthesis of TiO_2 nanoparticles and any other metal and metal oxide different NPs. The use of different parts of plants in the biosynthesis of TiO_2 nanoparticles and their applications holds immense potentials towards the environment. The source of the plant extract is known to influence the characteristics of the nanoparticles and hence its applications. This is because different extracts contain different concentrations and different types

of organic reducing agents and at same time different capping agents [16–18].

The genus *Kniphofia* (subfamily *Asphodeloideae*, family *Asphodelaceae*) comprises 70 species mainly confined to Africa with the center of diversity being South Africa [19], of which, seven occur in Ethiopia; among these seven species, five of them including *Kniphofia foliosa*, *Kniphofia hildebrandtii*, *Kniphofia isoetifolia*, *Kniphofia insignis*, and *Kniphofia schimperi* are endemic to Ethiopia [20]. Traditionally, the roots of *Kniphofia foliosa* have been used for the treatment of different ailments including menstrual pains, infertility, abdominal cramps, wounds, malaria, chest complaint, gonorrhea, and hepatitis [21]. In addition to its traditional medicinal usage for household remedy against various human ailments, the roots of *Kniphofia foliosa* extracts with various functional groups could also be used for the synthesis of TiO_2 NPs in order to exclude the addition of external stabilizing agents during synthesis process.

Antimicrobial resistance (AMR) is the ability of a microbe to resist the effects of medication that once could successfully treat the microbe. Bacterial resistance occurs as a result of either natural or acquired mechanism. Natural resistance results when the properties of bacteria inhibit the action of a certain antibiotics. As reported earlier, an antibiotic designed to attach to certain specific receptors on a bacterial cell is unable to act if the bacterial species does not have the receptors, while acquired resistance results due to change of bacterial species and its genetic makeup in such a manner that it decreases the action of antibiotics [22, 23]. During the last decades, a rapid increment in the development of new antibacterial inorganic and organic materials has been observed as consequence of the spread of antibiotic resistant infection disease, which has become a major issue in the current health care [15, 24]. Previously, several different researches were done on the antimicrobial activity of commercially available and chemically synthesized titanium oxide nanoparticles. But those methods are not environmentally friendly and at same time not cost effective. Biosynthesis of TiO_2 NPs using indigenous medicinal plant, root of *Kniphofia foliosa* extract, for *in vitro* antibacterial activity was not reported before this work. Therefore, the focus of the present study is biosynthesis of TiO_2 nanoparticles in different ratios using titanium tetrabutoxide as a precursor and *Kniphofia foliosa* root extract as a reducing and capping agent and then using the different ratios of biosynthesized TiO_2 nanoparticles to investigate its performance on both Gram-positive and Gram-negative human pathogen bacteria strains.

2. Methodology

2.1. Chemicals. Chemicals, reagents, and solvents used during this work include distilled water, absolute ethanol (99.9%, LabTech Chemicals), titanium tetrabutoxide (98%, Acros Organics), acetone (Sigma-Aldrich), dimethyl sulfoxide (DMSO, Sigma-Aldrich), and Müller-Hinton agar (Sigma-Aldrich). All these chemicals and reagents are of analytical grade and were used in this work without any further purification.



FIGURE 1: Schematic procedure for biosynthesis of TiO_2 NPs from titanium tetrabutoxide and ethanolic root extract of *Kniphofia foliosa*.

2.2. Extraction of the Root (Broth Solution). Enough amounts of roots of *Kniphofia foliosa* were collected and surface cleaned using distilled water several times and dried in a shaded room. The extraction was done by taking 5 grams of the root powder followed by addition of 200 mL of absolute ethanol as a solvent, and this was done using a 500 mL Erlenmeyer flask. And then, it was allowed to boil at $50^\circ C$ for about 35 minutes. The final extract of the solution was collected and stored at $4^\circ C$ within a refrigerator. The filtrate ethanolic root extract was used as a reducing and capping agent during the biosynthesis of TiO_2 NPs. TiO_2 NPs were biosynthesized within 1 : 2 (33.3 mL solution of titanium tetrabutoxide: 66.7 mL solution of root extract), 1 : 1 (50 mL solution of titanium tetrabutoxide: 50 mL solution of root extract), and 2 : 1 (66.7 mL solution of titanium tetrabutoxide: 33.3 mL solution of root extract) [15].

2.3. Biosynthesis of TiO_2 NPs. TiO_2 NPs were biosynthesized in different volume ratios by using 0.4 M of the precursor salt and ethanolic root extract of *Kniphofia foliosa* in a separate Erlenmeyer flask. In each case, the Erlenmeyer flask containing the two components was stirred for about 4 and a half hours without heating. Then, the solution was precipitated by adding a small drop of 1 M sodium hydroxide solution as a precipitating agent. Then, the formed TiO_2 NPs at different volume ratios were allowed to stay within a refrigerator overnight. The formed precipitate for each of the individual ratio was washed with absolute ethanol and distilled water 4 times following with centrifugation at 1000 rpm. At the end of the last centrifugation, the formed TiO_2 NPs were collected using a crucible ceramic dish and placed into a drying oven overnight at $100^\circ C$ [15]. Then, after conducting the thermal stability of the biosynthesized TiO_2 nanoparticles, it was calcined at $500^\circ C$ for about 3 and a half hours. Figure 1 shows the systematic biosynthetic procedure of TiO_2 NPs from its precursor (titanium tetrabutoxide) and ethanolic root extract of *Kniphofia foliosa* as a reducing and capping agent.

2.4. Characterization Techniques of Biosynthesized TiO_2 NPs. Thermal gravimetric analysis (TGA) of the biosynthesized NPs was carried out using a simultaneous differential thermal analysis DTA-TGA (DTG-60H, Shimadzu Co., Japan) and was used to determine the calcination temperature. The crystalline structure and the average crystalline size of the biosynthesized titanium oxide NPs were investigated using an X-ray diffractometer (XRD-7000, Shimadzu Co.,

Japan) and were recorded with 2θ from 10 to 80 using $CuK\alpha$ ($\lambda = 1.54056 \text{ \AA}$) radiation operated at 40 kV and 30 mA. Biosynthesized TiO_2 NPs were characterized by field emission scanning electron microscopy equipped with energy dispersive X-ray spectroscopy (FE-SEM, JEOL-JSM 6500F, made in Japan). The morphology was analyzed using high-resolution transmission electron microscopy (HRTEM, Tecnai F20 G2, Philips, Netherlands) at an accelerating voltage of 200 kV.

The absorption spectra of the biosynthesized TiO_2 NPs were recorded by using JASCO V-670 UV-Vis spectroscopy equipped with a diffuse reflectance attachment for powder samples in between a wavelength scan of 200 and 800 nm. TiO_2 NPs were characterized and recorded using Fourier transform infrared spectroscopy (FTIR, Perkin Elmer 65) to analyze and detect surface functional groups of the biosynthesized TiO_2 nanoparticles at the scanning range of $4000\text{--}400 \text{ cm}^{-1}$.

2.5. Antibacterial Studies

2.5.1. Preparation of Inoculums. Nutrient broth agar of 1.5 g was prepared within 100 mL of DH_2O and then was placed within four different conical flasks and sterilized. The prepared cultures were subcultured and were inoculated in nutrient broth and were kept on a rotary shaker at $35^\circ C \pm 2^\circ C$ for about 24 hours at 160 rpm.

2.5.2. Inoculation of Test Plates. Nutrient agar was prepared by taking 6 g nutrient agar and 0.8 g agar-agar followed by dissolving them within 100 mL of deionized water. The prepared agar suspension within 22 minutes was used to inoculate plates by dipping a sterile cotton wool swab into the suspension. Before applying the antibiotic disks, the plates were allowed to dry completely. The plates were incubated at $37^\circ C$ for about 16-18 hours in an incubator for bacteria and were checked for the zone of inhibition [25].

2.5.3. Disc Diffusion Method. The antibacterial activity of biosynthesized TiO_2 (1 : 2, 1 : 1, and 2 : 1 ratios) nanoparticles and that of ethanolic crude extract of roots of *Kniphofia foliosa* was investigated using the disc diffusion method using Müller-Hinton broth agar against both Gram-positive bacteria strains of *Staphylococcus aureus* and *Streptococcus pyogenes* and Gram-negative bacteria strains of *Escherichia coli* and *Klebsiella pneumoniae*.

Four bacterial cultures from each bacterial strains were maintained on nutrient Müller-Hinton agar at $37^\circ C$, and

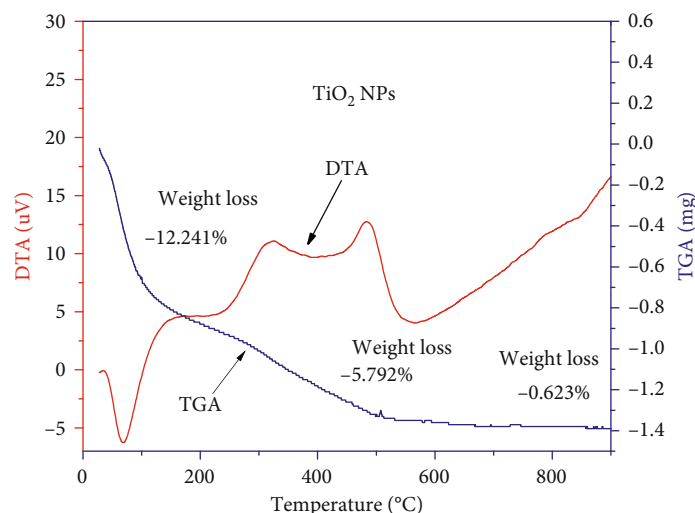


FIGURE 2: TGA-DTA analysis of as-synthesized titanium oxide NPs prepared from titanium tetrabutoxide and ethanolic root extract of *Kniphofia foliosa* in a 1:1 ratio.

the cultures were kept in appropriate media slants and stored at 4°C (to allow diffusion) until used. The plates were incubated at 37°C for 16–18 h in an incubator and were shaken gently to allow evenly mixing of bacteria cells and agar. Then, 35 mg from each of the three ratios of TiO₂ NPs (1:2, 1:1, and 2:1) was taken and dissolved within 1 mL of DMSO to obtain 35 mg/mL. From each different ratio, 80 µL was taken and saturated with discs (6 mm diameter) and incubated at 37°C for about 24 hours. In antibacterial testing against each strain, triplicate measurements were collected and the average of the triplicates was used in reporting the result.

The antibacterial activity of roots of *Kniphofia foliosa* extracted using ethanol (ethanol absolute; 99.9%) was investigated using the disc diffusion method. This was done by taking 50 mg of the root powder followed by addition of 25 mL ethanol and then was allowed to stay for about 72 hours until the required crude extract was obtained. The crude was filtered, the solvent was allowed to evaporate, and then, the remaining crude was checked both on Gram-positive and Gram-negative human pathogen bacteria strains. The antibacterial activity of both the biosynthesized TiO₂ nanoparticles and the crude extract was evaluated by measuring the diameter (mm) of the inhibition zone around the disc against the test organisms by using a ruler.

3. Results and Discussion

3.1. Thermal Gravimetric-Differential Thermal Analysis (TGA-DTA). Figure 2 shows TGA-DTA of synthesized TiO₂ NPs. Before calcination process was carried out, the thermal behavior of the as-biosynthesized TiO₂ nanoparticles was analyzed by means of thermogravimetric and differential thermal analysis. TGA curve shows weight loss of the biosynthesized sample whereas DTA curve indicates the energy gain or loss during the process.

Below 150°C, the weight loss was observed due to the removal of physically and chemically entrapped water molecules. In the temperature range of 150–350°C, the weight loss

also occurred due to the pyrolysis and carbonization of biomass [1].

Weight loss again continued up to 483°C associated with a strong exothermic peak in the DTA curve, which can be attributed to the vaporization of carbonized residues over the surface of the biosynthesized nanosample. Similar results related to the present study were also reported [14]. After 483°C up to 900°C, no considerable weight loss was observed; therefore, as a result of thermal analysis, 500°C was used as calcination temperature during this work.

3.2. X-Ray Diffraction (XRD) Analysis. Figure 3 shows XRD of TiO₂ NPs synthesized within three different volume ratios. The formation of biosynthesized TiO₂ NPs was also confirmed by X-ray diffraction measurements. The diffraction peaks were observed at 2θ values of $\approx 25.3, 38.0, 47.9, 53.2, 54.8862, 62.7, 70.2,$ and 75.0 along with their Miller index planes of (101), (004), (200), (105), (211), (204), (220), and (215), respectively. The analysis confirms that the biosynthesized titanium oxide nanoparticles are in a tetragonal crystal structure without any impurities within the detection limits of XRD instrument and within the scanned region done from 10° to 80°. As the width of the peak increases, the size of the particle decreases, which resembles that the present biosynthesized TiO₂ material is within the range of nano [26].

The average crystalline size for the different kinds of TiO₂ NPs was estimated as 10.2, 8.2, and 8.5 nm for the 1:2, 1:1, and 2:1 ratios, respectively. The average crystallite size of TiO₂ nanoparticles synthesized within a 1:1 ratio has a relatively smaller particle size of 8.2 nm as compared to the average crystalline size of 8.5 nm for the case of a 2:1 ratio. This is due to the fact that the greater amount of the extract used during the synthesis process results in more capping agents/stabilizing agents that in turn effectively stabilize the biosynthesized TiO₂ nanoparticles during the synthesis process. The peaks of both of the XRD spectra are in good agreement with the literature reported before (19). As it can be observed for the XRD spectrum (a), TiO₂ (1:2) NPs losses

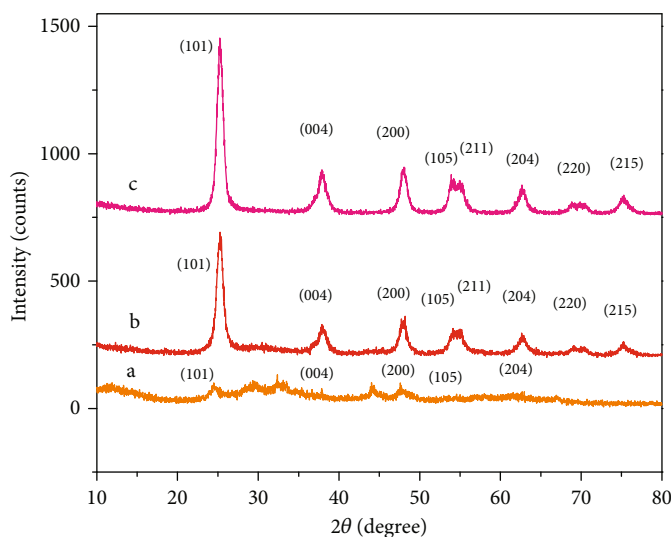


FIGURE 3: XRD spectra of TiO_2 NPs biosynthesized in (a) 1:2, (b) 1:1, and (c) 2:1 ratios of titanium tetrabutoxide and root extract of *Kniphofia foliosa*.

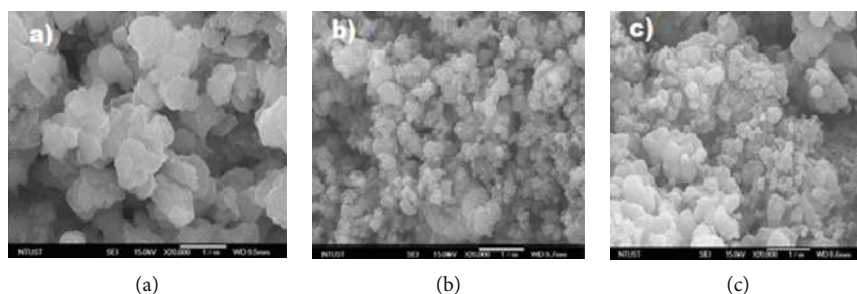


FIGURE 4: SEM images of TiO_2 NPs biosynthesized in (a) 1:2, (b) 1:1, and (c) 2:1 ratios of titanium tetrabutoxide and root extract of *Kniphofia foliosa*.

their crystalline nature due to the addition of an excessive amount of the root extract of *Kniphofia foliosa* beyond the coating surface of TiO_2 NPs.

3.3. Scanning Electron Microscopy-Energy Dispersive Spectroscopy (SEM-EDS). Figure 4 shows SEM images of TiO_2 NPs synthesized within three different volume ratios. SEM images revealed that the biosynthesized TiO_2 NPs were found to be spherical in shape with distinct edges. SEM images also revealed the increase of particle size with the increase of ethanolic root extract of *Kniphofia foliosa*. Moreover, the uniformity of the SEM image in case of TiO_2 (1:1 and 2:1) relative to TiO_2 (1:2) ratio implies the well association of biomolecules obtained from the root extract with TiO_2 nanoparticles during the synthesis process; and the presence of the root extract coats the surface of the TiO_2 nanoparticles thus preventing from aggregation.

As it can be shown from Figure 4(a), the particles show agglomeration which results due to the presence of excess amount of root extract of *Kniphofia foliosa*, which was beyond the coating surface of TiO_2 NPs [27]. This image was observed within the magnification of $20\ \mu\text{m}$.

To gain a further insight into the features of the bio-synthesized TiO_2 nanoparticles, the analysis was performed using EDS techniques. The absence of any foreign materials other than the required elements (titanium and oxygen) indicates the elimination of water molecules, ethanol molecules, and other organic residues during the centrifugation, drying, and calcination steps; this reveals that the synthesized TiO_2 NPs were pure as supported by the XRD analysis results [28].

EDS analysis results (Figure 5) clearly showed that the peaks due to Ti were highly intense, and at the same time, the result showed low intense oxygen peaks which may be due to the dissociation of the precursor compound (titanium tetrabutoxide) used during the synthesis of process. EDS also revealed the formation of nonstoichiometry TiO_2 NPs with oxygen vacancy, which leads to the better performance for the desired application (in the present case for antibacterial activity).

3.4. Transmission Electron Microscopy (TEM) Analysis. Figure 6 revealed TEM image, SAED pattern, and HRTME results of the biosynthesized TiO_2 (1:1) NPs. TEM analysis was carried out to ascertain and gain further information

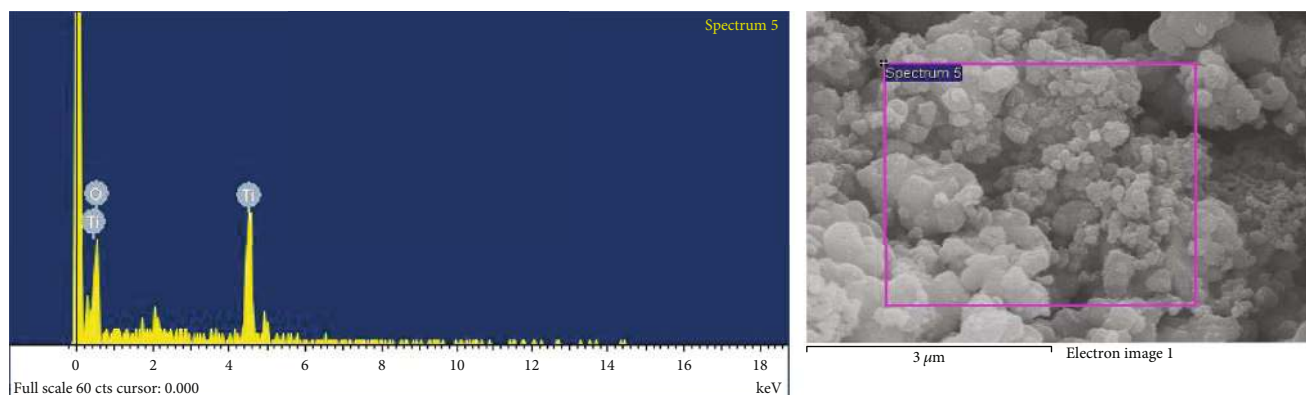


FIGURE 5: EDS analysis (left) of biosynthesized TiO_2 NPs (1 : 1) from the selected area in SEM image (right).

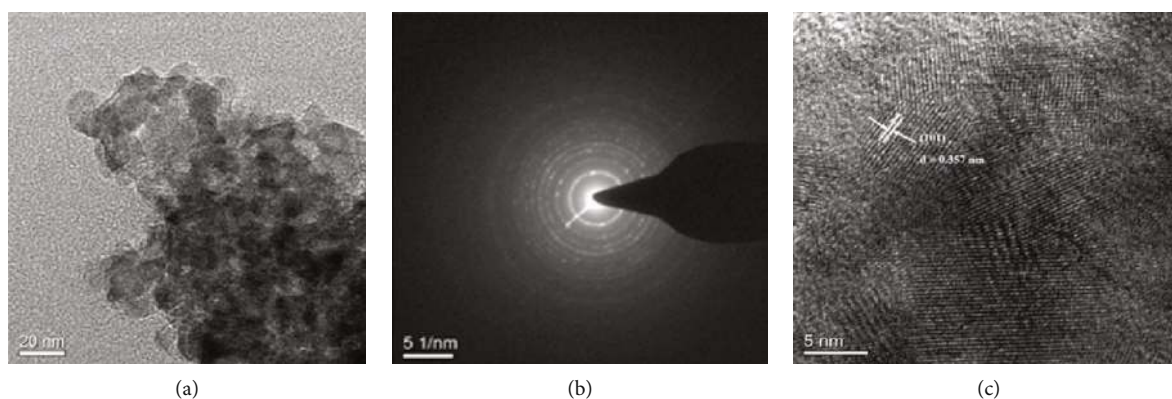


FIGURE 6: (a) TEM image of TiO_2 NPs, (b) SAED pattern of TiO_2 NPs, and (c) HRTEM image of TiO_2 NPs biosynthesized from titanium tetrabutoxide and ethanolic root extract of *Kniphofia foliosa* in a 1 : 1 ratio.

about the biosynthesized TiO_2 NPs. TEM image exhibits that the morphology of the biosynthesized titanium oxide nanoparticles possesses a spherical/sphere-like structure in shape without any agglomeration.

The TEM image also reveals that the biosynthesized anatase TiO_2 nanoparticles were found to have good crystalline nature, as it was also supported by the XRD analysis results [15]. The crystalline nature was also confirmed by the selected area electron diffraction (SAED) pattern with bright circular spots corresponding to (101), (004), (200), (105), (211), (204), (220), and (215), respectively, planes of the anatase lattice of biosynthesized TiO_2 nanoparticles [16].

The image in Figure 6(c) with higher magnification shows the high-resolution transmission electron microscope (HRTEM) of anatase TiO_2 NPs. The particles with a fringe width of 0.357 nm were confirmed to be anatase form of biosynthesized TiO_2 (101) nanoparticles. The lattice fringes also clearly indicate that the particles are nanocrystalline with an anatase phase form, which is also confirmed by the XRD analysis result and from the SAED pattern analysis.

3.5. Ultraviolet-Visible (UV-Vis) Analysis. Figure 7 shows the UV-Vis absorption spectrum and the Tauc plot spectrum for the different kinds of biosynthesized TiO_2 NPs. The absorption spectra of the biosynthesized TiO_2 NPs reveal the reduc-

tion process and formation of TiO_2 , which shows excellent agreement with those reported in literatures previously. The bandgap energy was determined based on the numerical derivative of the optical absorption coefficient using Tauc's plot method and was found to be 3.34, 3.32, and 3.37 eV for the 1:2, 1:1, and 2:1 volume ratios of Ti precursor salt and root extract, respectively. The variation in the E_g for the different kinds of biosynthesized TiO_2 NPs is due to the variation in volume ratio between Ti precursor salt and the root extract that leads the biosynthesized TiO_2 NPs to absorb at different regions of UV-Vis light.

Broadening of the spectrum indicates the polydispersed nature of the biosynthesized nanoparticles and the red shift of the absorption curve results in the reduction of the band-gap energy.

3.6. Fourier Transform Infrared (FTIR) Spectroscopy. The FTIR spectrum of dried *Kniphofia foliosa* plant extract powder and biosynthesized titanium oxide nanoparticles were indicated by Figures 8(a) and 8(b), respectively. Absorption bands at 3419.46, 2926.88, 1635.14, 1319.59, 1038, and 780.44 cm^{-1} are due to O-H bond stretching, C-H bond stretching of alkanes, C=O bond stretching of carbonyl groups/C=C bond stretching at α,β -unsaturated ketone, C-C bond stretching at aromatic ring, C-O bond bending

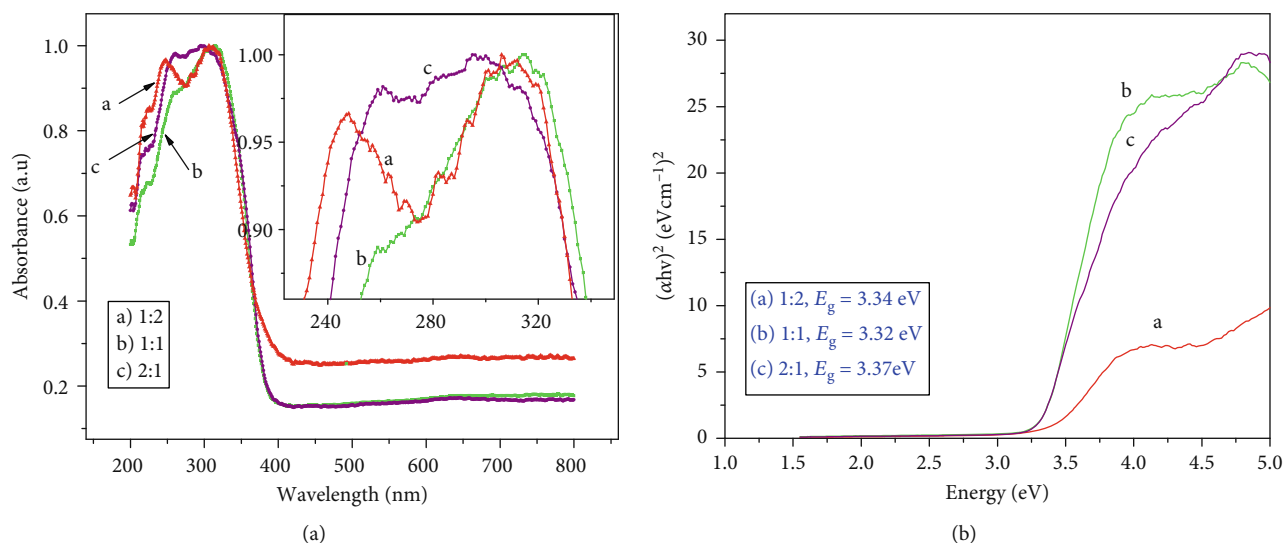


FIGURE 7: (a) UV-Vis absorption spectra and (b) Tauc plot of TiO₂ NPs synthesized from titanium tetrabutoxide and extract of root of *Kniphofia foliosa* in a volume ratio of 1:2, 1:1, and 2:1, respectively.

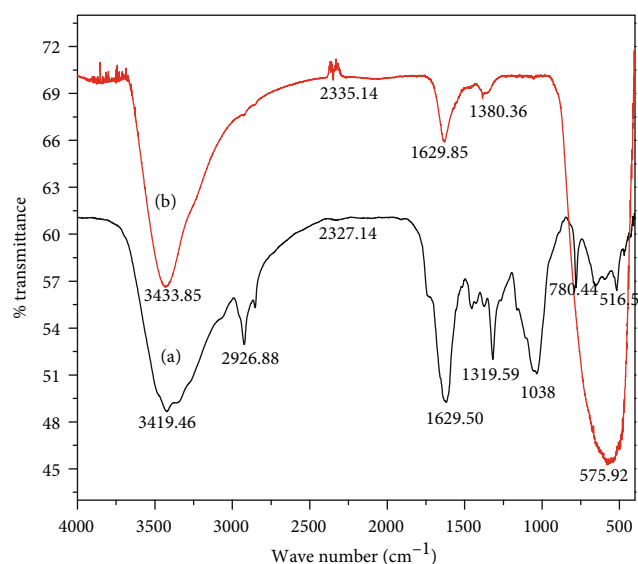


FIGURE 8: FTIR spectra of (a) dried *Kniphofia foliosa* plant extract powder and (b) biosynthesized TiO₂ NPs (after calcination).

vibration on phenolic compound, C-O bond stretching of the hydroxyl group, and out of plane C-H bending at aromatic ring, respectively, indicating and showing the presence of organic compounds such as knipholone anthrone, anthraquinone, and chrysophanol [29]. In Figure 8(b), the broad absorption band observed at 3433.85 cm⁻¹ represents O-H bond stretching due to adsorbed moisture at the surface of TiO₂ NPs, and the weak absorption band at 2335.14 cm⁻¹ is due to C=O bond stretching that could be emanated from the presence of adsorbed carbon dioxide on the surface of NPs. The absorption band at 1629.58 cm⁻¹ also was due to carbon dioxide and/or due to O-H bending of molecularly adsorbed water on the surface of the synthesized material shown in Figure 8(b) [30].

The broad band centered at 567.13 cm⁻¹ represents a characteristic peak of Ti-O-Ti bending mode of vibration which confirms the formation of metal oxygen bonding [31, 32]. The absence of bands at 2926.88, 1635.14, 1319.59, 1038, and 780.44 cm⁻¹ in Figure 8(b) shows that organic molecules used during synthesis have been removed from the TiO₂ NPs upon calcination above 500°C.

3.7. Antibacterial Study Analysis. The antibacterial activity of the biosynthesized TiO₂ nanoparticles and that of the ethanolic crude extract of the roots of *Kniphofia foliosa* was investigated using the disc diffusion method. Table 1 shows the antibacterial activity of TiO₂ nanoparticles biosynthesized within 1:2, 1:1, and 2:1 ratios, which shows the antibacterial zone of inhibition between 8 and 6 mm at the concentration of 35 mg/mL against *Staphylococcus aureus*, *Escherichia coli*, *Klebsiella pneumonia*, and *Streptococcus pyogenes*.

Among the different ratios of the biosynthesized TiO₂ NPs, TiO₂ (1:1) NPs show better performing antibacterial activity as compared to the remaining two ratios. This might be due to the smaller average crystalline size; and in addition to this, the enhancement is also due to the more uniform spherical shape of TiO₂ NPs as it can be seen from its SEM image. From the present study, it is clearly evident that the greater inhibitory action of green synthesized TiO₂ (1:1) nanoparticles depends not only on average crystalline size of the nanoparticles but also on the difference in volume of capping agents obtained from the root extract of *Kniphofia foliosa*. Biosynthesized TiO₂ NPs within a volume ratio of 1:2 show resistant towards *S. aureus*, *S. pyogenes*, and *K. pneumonia* bacteria strains except *E. coli*. This might be because of that the morphology of the biosynthesized TiO₂ NPs shows agglomeration which results in lowering the *in vitro* antibacterial activity. This might also be due to the larger average crystalline nature of the formed nanoparticles in its XRD spectrum as compared to the other ratios.

The antibacterial activity of the crude ethanolic root extract of *Kniphofia foliosa* was investigated by measuring

TABLE 1: Antibacterial activity of TiO₂ NPs biosynthesized within 1:2, 1:1, and 2:1 ratios of titanium tetrabutoxide and root extract of *Kniphofia foliosa*, against *Staphylococcus aureus*, *Escherichia coli*, *Klebsiella pneumonia*, and *Streptococcus pyogenes* bacteria strains (at the concentration of 35 mg/mL of TiO₂ NPs).

Precursor salt: plant extract ratio	<i>S. aureus</i> (mm)	<i>S. pyogenes</i> (mm)	<i>E. coli</i> (mm)	<i>K. pneumonia</i> (mm)
TiO ₂ (1:2)	6	6	7	6
TiO ₂ (1:1)	8	7	8	8
TiO ₂ (2:1)	7	6	7	7
DMSO	6	6	6	6
Gentamicin (+ve) control	6	6	9	10

the zone of inhibition and found to be 10, 10, 6, and 6 mm for the *S. aureus*, *S. pyogenes*, *E. coli*, and *K. pneumonia*, respectively. The crude ethanolic root extract of *Kniphofia foliosa* shows the best antibacterial activity against Gram-positive bacteria (*S. aureus* and *S. pyogenes*). This indicates that the ethanolic crude extract of the plant was more sensitive against Gram-positive bacteria than Gram-negative bacteria [27]. The zones of inhibition by ethanolic root extract of *Kniphofia foliosa* against Gram-negative bacteria were smaller than that of Gram-positive bacteria. This is because Gram-negative bacteria possess additional external cell membrane/double cell membrane that allows them to resist.

Green synthesized TiO₂ NPs show antibacterial activity because biomolecules obtained from the root extract of *Kniphofia foliosa* are giving excess electron to TiO₂ and result in the formation of superoxide radicals O₂⁻, and the superoxide radicals produce reactive oxygen species (ROS) in bacterial cell. That ROS is used to break the bacterial cell membrane. As the superoxide radical production increased, ROS production also increased. These are all of the reasons for electron production from TiO₂ nanoparticles, and as a result, TiO₂ NPs show antibacterial activity against both Gram-negative and Gram-positive bacteria strains [33].

According to several studies, it is believed that metal oxides carry positive charge while bacteria carry negative charges; this causes electrostatic attraction between bacterial cells and metal oxide NPs, which leads to oxidation and finally death of microorganisms [33]. Nanomaterials also could deactivate the cellular enzymes and DNA by coordinating to the electron-donating group. Therefore, this result showed that TiO₂ nanoparticles were effective for inhibiting Gram-positive and Gram-negative bacteria. As it can be observed from Table 1, the antibacterial activity of the synthesized TiO₂ NPs towards Gram-positive bacteria strains is low. This might be due to the nature of the bacteria strains that resist towards the synthesized material. The antibacterial effect of biosynthesized TiO₂ nanoparticles may be due to its small size, more uniform spherical shape, and more active sites of TiO₂ NPs. This also implies that TiO₂ NPs may destroy the outer membrane of the bacterial cell, directly leading to the leakage of minerals, proteins, and genetic materials, causing cell death of the corresponding human pathogen bacteria.

4. Conclusion

In this work, TiO₂ NPs were successfully biosynthesized using titanium tetrabutoxide as a precursor in the presence

of *Kniphofia foliosa* root extract within different ratios. More crystalline nature and best performing TiO₂ NPs were obtained when it was biosynthesized within a 1:1 ratio. The biosynthesized TiO₂ NPs were characterized using different instruments. The particles were found to be thermally stable above 500°C. Crystalline analysis showed the average crystalline size as 10.2, 8.2, and 8.5 nm for 1:2, 1:1, and 2:1, respectively. SEM reveals the morphology as spherical, and EDS analysis also indicates presence of the elements such as Ti and O only. TEM image confirmed the spherical morphology of the biosynthesized TiO₂ NPs, and HRTEM analysis proves that the lattice spacing of 0.357 nm confirms (101) plane of anatase TiO₂ NPs. The bandgap was calculated in the range of 3.32-3.37 eV. Functional group analysis indicates the presence of various capping and stabilizing agents. The *in vitro* antibacterial activity of both the biosynthesized three ratios of TiO₂ NPs and ethanolic crude root extract of *Kniphofia foliosa* was investigated. Among the different ratios of TiO₂ NPs, TiO₂ (1:1) have better performing antibacterial activity. This is due to its small average crystalline size, uniform spherical shape, and large surface region, which creates electronic effects, and these effects can increase the binding strength of the nanoparticles with the bacteria cell membrane. Ethanolic crude root extract of *Kniphofia foliosa* has a better activity against *S. aureus* and *S. pyogenes*.

Data Availability

The data of UV-Visible absorption spectra, FTIR spectra, XRD Analysis, SEM, EDS, TEM images, HRTEM images, SAED patterns, and antibacterial activity used to support the findings of this study are included within the article; and also can be released from corresponding author upon application to the Review Board of Hindawi (Journal of Nanomaterials).

Disclosure

The funder, Adama Science and Technology University, has not been involved in the editing, approval, or decision to publish this manuscript.

Conflicts of Interest

The authors declare that they have no conflicts of interest.

Acknowledgments

The authors acknowledge Adama Science and Technology University (ASTU) for supporting this project through ASTU's 12th cycle research grant successfully. The authors extend their thanks to the department of applied chemistry and department of materials science and engineering at Adama Science and Technology University for providing facilities such as a UV-visible spectrophotometer, thermal analyzer, and XRD. The Department of Chemistry at Addis Ababa University was also thanked by authors for allowing FT-IR analysis. For SEM, EDS, and TEM analysis, the authors acknowledge the Department of Materials Science and Engineering, National Taiwan University of Science and Technology (NTUST), Taiwan.

References

- [1] M. Vijaylaxmee, R. Sharma, D. J. Nakuleshawar, and D. K. Gupta, "A review on green synthesis of nanoparticles and evaluation of antimicrobial activity," *International Journal of Green and Herbal Chemistry*, vol. 3, no. 1, pp. 081–094, 2014.
- [2] T. Rasheed, M. Bilal, C. Li, F. Nabeel, M. Khalid, and H. M. N. Iqbal, "Catalytic potential of bio-synthesized silver nanoparticles using *Convolvulus arvensis* extract for the degradation of environmental pollutants," *Journal of Photochemistry and Photobiology B: Biology*, vol. 181, pp. 44–52, 2018.
- [3] L. Rotimi, M. O. Ojemaye, O. O. Okoh, A. Sadimenko, and A. I. Okoh, "Synthesis, characterization, antimalarial, antitypanocidal and antimicrobial properties of gold nanoparticle," *Green Chemistry Letters and Reviews*, vol. 12, no. 1, pp. 61–68, 2019.
- [4] T. Rasheed, M. Bilal, H. M. N. Iqbal, and C. Li, "Green biosynthesis of silver nanoparticles using leaves extract of *Artemisia vulgaris* and their potential biomedical applications," *Colloids and Surfaces B: Biointerfaces*, vol. 158, pp. 408–415, 2017.
- [5] R. Larayetan, M. O. Ojemaye, O. O. Okoh, and A. I. Okoh, "Silver nanoparticles mediated by *Callistemon citrinus* extracts and their antimalaria, antitypanosoma and antibacterial efficacy," *Journal of Molecular Liquids*, vol. 273, pp. 615–625, 2019.
- [6] M. Herrera, P. Carrión, P. Baca, J. Liébana, and A. Castillo, "In vitro antibacterial activity of glass-ionomer cements," *Journal of Microbiology*, vol. 104, no. 21, pp. 141–148, 2001.
- [7] M. R. Hoffmann, S. T. Martin, W. Choi, and D. W. Bahnemann, "Environmental applications of semiconductor photocatalysis," *Chemical Reviews*, vol. 95, no. 1, pp. 69–96, 1995.
- [8] O. Carp, C. L. Huisman, and A. Relle, "Photoinduced reactivity of titanium dioxide," *Progress in Solid State Chemistry*, vol. 32, no. 1–2, pp. 33–177, 2004.
- [9] Y. Y. Loo, B. W. Chieng, M. Nishibuchi, and S. Radu, "Synthesis of nanoparticles by using tea leaf extract from *Camellia sinensis*," *International Journal of Nanomedicine*, vol. 2012, no. 7, pp. 4263–4267, 2012.
- [10] J. Luo, J. Wu, Z. Liu, Z. Li, and L. Deng, "Controlled synthesis of porous Co_3O_4 nanostructures for efficient electrochemical sensing of glucose," *Journal of Nanomaterials*, vol. 2019, Article ID 8346251, 7 pages, 2019.
- [11] L. Rodríguez-Sánchez, M. C. Blanco, and M. A. López-Quintela, "Electrochemical synthesis of silver nanoparticles," *Journal of Physical Chemistry*, vol. 104, no. 41, pp. 9683–9688, 2000.
- [12] M. Hudlikar, S. Joglekar, M. Dhaygude, and K. Kodam, "Green synthesis of TiO_2 nanoparticles by using aqueous extract of *Jatropha curcas L. latex*," *Materials Letters*, vol. 75, no. 1, pp. 196–199, 2012.
- [13] G. Rajakumar, A. A. Rahuman, B. Priyamvada, V. G. Khanna, D. K. Kumar, and P. J. Sujin, "Eclipta prostrata leaf aqueous extract mediated synthesis of titanium dioxide nanoparticles," *Materials Letters*, vol. 68, no. 1, pp. 115–117, 2012.
- [14] D. Ramimoghdam, S. Bagheri, and S. B. Abd Hamid, "Bio-templated Synthesis of Anatase Titanium Dioxide Nanoparticles via Lignocellulosic Waste Material," *BioMed Research International*, vol. 2014, Article ID 205636, 7 pages, 2014.
- [15] T. Santhoshkumar, A. A. Rahuman, C. Jayaseelan et al., "Green synthesis of titanium dioxide nanoparticles using *Psidium guajava* extract and its antibacterial and antioxidant properties," *Asian Pacific Journal of Tropical Medicine*, vol. 7, no. 12, pp. 968–976, 2014.
- [16] S. Baker, D. Rakshith, K. S. Kavitha et al., "Plants: Emerging as Nanofactories Towards Facile Route in Synthesis of Nanoparticles," *Bioimpacts*, vol. 3, no. 3, pp. 111–117, 2013.
- [17] K. S. Mukunthan and S. Balaji, "Cashew apple juice (*Anacardium occidentale L.*) speeds up the synthesis of silver nanoparticles," *International Journal of Green Nanotechnology*, vol. 4, no. 2, pp. 71–79, 2012.
- [18] R. Shashikant Kuchekar, P. Monali Patil, B. Vishwas, H. Gaikwad, and S. Han, "Synthesis and characterization of silver nanoparticles using *Azadirachta indica* (Neem) leaf extract," *International Journal of Engineering Science Invention*, vol. 6, no. 4, pp. 47–55, 2017.
- [19] R. M. T. Dahlgren, H. T. Clifford, and P. F. Yeo, "The families of the monocotyledons," *Plant Systematics and Evolution*, vol. 167, no. 1, pp. 75–86, 1989.
- [20] C. Whitehouse, "Asphodelaceae: flora of tropical East Africa, Beentje, H.J.A. first edition," *Botany and Plant Science*, vol. 47, no. 1, pp. 1–40, 2001.
- [21] M. Giday, Z. Asfaw, and Z. Woldu, "Medicinal plants of the Meinit ethnic group of Ethiopia: an ethnobotanical study," *Journal of Ethnopharmacology*, vol. 124, no. 3, pp. 513–521, 2009.
- [22] A. M. Amanulla and R. Sundara, "Green synthesis of TiO_2 nanoparticles using orange peel extract for antibacterial, cytotoxicity and humidity sensor applications," *Materials Today*, vol. 8, pp. 323–331, 2019.
- [23] R. Ahmad and M. Sardar, " TiO_2 nanoparticles as an antibacterial agents against *E. coli*," *International Journal of Innovative Research in Science and Engineering Technology*, vol. 2, no. 8, pp. 3569–3574, 2013.
- [24] R. Chauhan, A. Kumar, and J. Abraham, "A biological approach to the synthesis of silver nanoparticles with *Streptomyces sp* JAR1 and its antimicrobial activity," *Scientia Pharmaceutica*, vol. 81, no. 2, pp. 607–621, 2013.
- [25] D. Sritabutra, M. Soonwera, S. Waltanachanobon, and S. Pongjai, "Evaluation of herbal essential oil as repellents against *Aedes aegypti* (L.) and *Anopheles dirus* Peyton & Harrison," *Asian Pacific Journal of Tropical Biomedicine*, vol. 1, no. 1, pp. S124–S128, 2011.
- [26] S. Marimuthu, A. A. Rahuman, C. Jayaseelan et al., "Acaricidal activity of synthesized titanium dioxide nanoparticles using *Calotropis gigantea* against *Rhipicephalus microplus* and

- Haemaphysalis bispinosa,” *Asian Pacific Journal of Tropical Medicine*, vol. 6, no. 9, pp. 682–688, 2013.
- [27] C. Malarkodi, K. Chitra, S. Rajeshkumar et al., “Novel eco-friendly synthesis of titanium oxide nanoparticles by using Planomicrobium sp. and its antimicrobial evaluation,” *Der Pharmacia Sinica*, vol. 4, no. 3, pp. 59–66, 2013.
- [28] D. C. L. Vasconcelos, V. C. Costa, E. H. M. Nunes, A. C. S. Sabioni, M. Gasparon, and W. L. Vasconcelos, “Infrared spectroscopy of titania sol-gel coatings on 316L stainless steel,” *Materials Sciences and Applications*, vol. 2, no. 10, pp. 1375–1382, 2011.
- [29] A. Yenesew, E. Dagne, M. Müller, and W. Steglich, “An anthrone, an anthraquinone and two oxanthrones from *Kniphofia foliosa*,” *Phytochemistry*, vol. 37, no. 2, pp. 525–528, 1994.
- [30] K. Coenen, F. Gallucci, B. Mezari, E. Hensen, and M. van Sint Annaland, “An in-situ IR study on the adsorption of CO₂ and H₂O on hydrotalcites,” *Journal of CO₂ Utilization*, vol. 24, pp. 228–239, 2018.
- [31] A. M. Peiró, J. Peral, C. Domingo, X. Domènech, and J. A. Ayllón, “Low-temperature deposition of TiO₂ Thin films with photocatalytic activity from colloidal anatase aqueous solutions,” *Chemistry of Materials*, vol. 13, no. 8, pp. 2567–2573, 2001.
- [32] G. B. Reddy, A. Madhusudhan, D. Ramakrishna, D. Ayodhya, M. Venkatesham, and G. Veerabhadram, “Green chemistry approach for the synthesis of gold nanoparticles with gum kondagogu: characterization, catalytic and antibacterial activity,” *Journal of Nanostructure in Chemistry*, vol. 5, no. 2, pp. 185–193, 2015.
- [33] H. Zhang and G. Chen, “Potent antibacterial activities of Ag/TiO₂ nanocomposite powders synthesized by a one-pot sol-gel method,” *Environmental Science and Technology*, vol. 43, no. 8, pp. 2905–2910, 2009.